REVIEW ARTICLE   OPEN

Review of corrosion interactions between different materials relevant to disposal of high-level nuclear waste

Xiaolei Guo [1 ✉], Stephane Gin [2] and Gerald S. Frankel [1]

This review covers the corrosion interactions between different materials that are relevant to the disposal of high-level nuclear waste, in particular the waste forms and containers. The materials of interest are borosilicate glass, crystalline ceramics, metal alloys, and any corrosion products that might form. The available data show that these interactions depend on the structure, chemistry, thermodynamic history, and proximity of the materials in contact, as well as the environmental attributes, such as temperature, solution chemistry, and radiation. Several key mechanisms that govern these interactions are highlighted. Scientific gaps and open questions are summarized and discussed.

INTRODUCTION

In many countries, the current plan for the disposal of high level waste (HLW) includes mixing the radionuclides with aluminoborosilicate glass and heating them to a temperature exceeding the glass melt temperature, which is typically over 1000 °C[1–3]. The melted glass is subsequently cast into stainless steel (SS) canisters and cooled to room temperature, forming a stable solid-state glass waste form[2]. The waste that cannot be properly handled with glass, such as the semi-volatile ^{129}I and ^{99}Tc, can be immobilized with other waste forms including metals or crystalline ceramics and then encapsulated in metallic canisters. Worldwide, HLW and spent nuclear fuel will be emplaced in deep geological repositories where the radioactive materials must be safely isolated from the environment for very long periods, on the order of 10^6 yr. The design of repository varies from country to country, due primarily to the different nature of the waste and geochemical environment. Here we briefly describe three repository scenarios: those from U.S., France, and Belgium. A comparison of the general repository data for these three countries is given in Table 1.

In the U.S. Yucca Mountain program, the vitrified HLW is stored in SS316 canisters with an outer diameter of ~61.0 cm and a wall thickness of ~1.3 cm[4,5]. As shown in Fig. 1, five of these small-diameter canisters with HLW along with another canister with spent nuclear fuel will be placed into a two-layered canister, including an inner cylinder made from SS316 (~5 cm in thickness) and an outer cylinder made from Alloy 22 (~2.5 cm in thickness)[6]. Both the SS316 and Alloy 22 are highly resistant to general corrosion but are susceptible to localized corrosion, especially in Cl$^-$ containing solutions[7,8]. As a result, there will be a considerable amount of metals surrounding the waste forms to ensure structure stability and safety. The volume for each of the small-diameter canister alone is about 9% of the volume of waste encapsulated inside. Therefore, the compatibility of the waste forms with the metallic canister should be a topic of interest. Apart from the SS container and Alloy 22 overpack, the engineered barrier for Yucca Mountain repository also includes a titanium drip shield that will be used to prevent underground water from dripping onto the waste packages (Fig. 1). No back-fill materials will be used after the

waste packages are emplaced. Different than most other countries, the Yucca Mountain repository is constructed in an unsaturated zone above the water table, so the geochemical environment is oxidizing in nature[9]. Although the repository is located in a desert, the repository site contains pore water[10] and structure water from zeolites[9]. Since both water and oxygen are present, corrosion could be a problem during the long-term storage of the waste.

The French Cigéo program describes a deep geological repository that will be built at the Meuse/Haute-Marne site, which is within a saturated zone under the water table and 500 m below the surface[11]. In this program, the HLW is also mixed with glass frit, then molten at 1050 °C in a hot crucible melter and poured into SS (AISI 309S) canisters. Carbon steel (CS) overpacks made from forged steel P285NH with a wall thickness of 6.5 cm (Fig. 2a) will be used for the confinement of the SS canister containing vitrified HLW. A micro-tunnel casing made from a different CS (API 5L X65 grade) with a wall thickness of 2.5 cm will be applied surrounding the CS overpack and emplaced in the drift (Fig. 2b)[12]. These waste packages will subsequently be embedded in filling materials (cement and bentonite mixture) with a wall thickness of about 10 cm, Fig. 2c. The selection of CS as the overpack material was based on the consideration that CS tends to corrode uniformly under the conditions prevailing at this repository, so the corrosion rate is more predictable compared to the localized corrosion[13]. After deposition of the waste package, the repository environment will evolve from a hot and humid oxic environment to an anoxic environment re-saturated with groundwater at the geothermal temperature[12]. Similar to the U.S. program, each waste package contains a greater amount of encapsulant metal (1500 kg) than the nuclear waste glass within (400 kg)[14].

The Belgian repository will be constructed in the midplane of the Boom Clay, which is also within the saturated zone 240 m below the surface[15]. An anoxic repository environment is expected as the oxygen introduced by the initial construction of the repository will be gradually consumed[16,17]. A supercontainer design was proposed in this program. As shown in Fig. 3, the SS canister[18] containing vitrified HLW will be surrounded by a CS overpack[19] with a wall thickness of 3 cm and then lined with a ~70 cm thick concrete buffer[20,21]. The alkaline environment

^{1}Department of Materials Science and Engineering, Ohio State University, Columbus, OH 43210, USA. ^{2}CEA, DEN, ISEC, DE2D, University of Montpellier, Marcoule, F-30207 Bagnols sur Cèze, France. ✉email: guo.237@buckeyemail.osu.edu

Table 1. Comparison of general HLW repository data for U.S., France, and Belgium.

Country	U.S.	France	Belgium
Existing HLW glass (2012)	6700 tons	7700 tons	650 tons
Origin	Defense waste 93% (by mass) + spent fuel 7%	Primarily spent fuel	Spent fuel
(Potential) repository site	Yucca Mountain	Meuse/Haute-Marne	Mol
Disposal concept	Glass + SS canister + SS and Alloy 22 overpack + Ti drip shield	Glass + SS canister + CS overpack and casing + filling materials (cement and bentonite mixture)	Glass + SS canister + CS overpack + concrete buffer + SS envelope + cement backfill
Dominant geochemical condition	Oxic	Anoxic	Anoxic

Part of the data was reproduced from Gin et al.[2]. CS and SS stand for carbon steel and stainless steel, respectively.
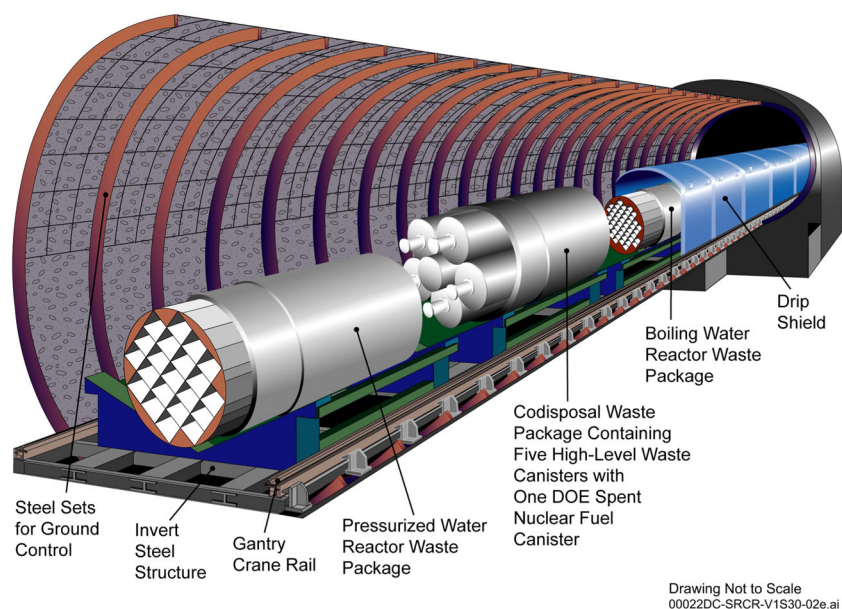
Fig. 1 Schematic illustration of in-drift placement of waste packages at the potential U.S. Yucca Mountain repository. Source U.S. Department of Energy.

conferred by the concrete can promote the formation of a stable passive film on the surface of the CS, leading to a low corrosion rate of the CS when aggressive species such as Cl^- are absent. The concrete block may be fitted into an additional container made from SS with a wall thickness of a few mm. The void space between the disposal gallery and SS envelope will be backfilled with cement-based materials following the waste emplacement.

After the metallic containers are emplaced in a repository, corrosion will be possible during a long heating and cooling cycle[22]. In the oxic environment at the U.S. repository, for example, underground water may progressively breach the Alloy 22 and then the SS canisters, mostly likely via localized corrosion[23,24], and eventually reach the encapsulated glass/ceramic waste forms. In an anoxic environment, such as the French and Belgian repositories, the CS overpack may be incrementally consumed by general corrosion assuming that aggressive species will be absent or below the threshold concentration[25], after which, however, the encapsulated SS canister may also be breached by localized corrosion. Therefore, it is crucial to understand the corrosion of each individual material involved in this process, including the metallic canisters, glass, and ceramic waste forms. Furthermore, the coupled corrosion interactions between these materials should also be taken into account. Over the past four

decades, efforts have been made to assess this nearfield corrosion interaction between materials and some key understanding has been achieved, yet no comprehensive review exists in the literature on this topic. Thus, in this article, we review the important studies that have contributed to the current understanding of the corrosion interaction between materials relevant to nuclear waste storage. It should be noted that although other materials can be present in the nearfield, including concrete, backfill clay, space fillers, etc., this review focuses primarily on glass, crystalline ceramics, metals, and their corrosion products. Since these corrosion interactions primarily depend on the material and environment, this review is organized by different material couples and the corresponding environment is specified for each study.

Glass and carbon steel

Low alloy carbon steel (CS) is a candidate overpack material proposed by several countries including France, Spain, and Belgium to enclose the glass-containing SS canister[13,26]. In general, CS has a higher corrosion rate compared to corrosion-resistant alloys (CRAs), such as SS and Alloy 22. Additionally, CS typically undergoes general corrosion in neutral and acidic environments, so it is easier to estimate the canister lifetime from
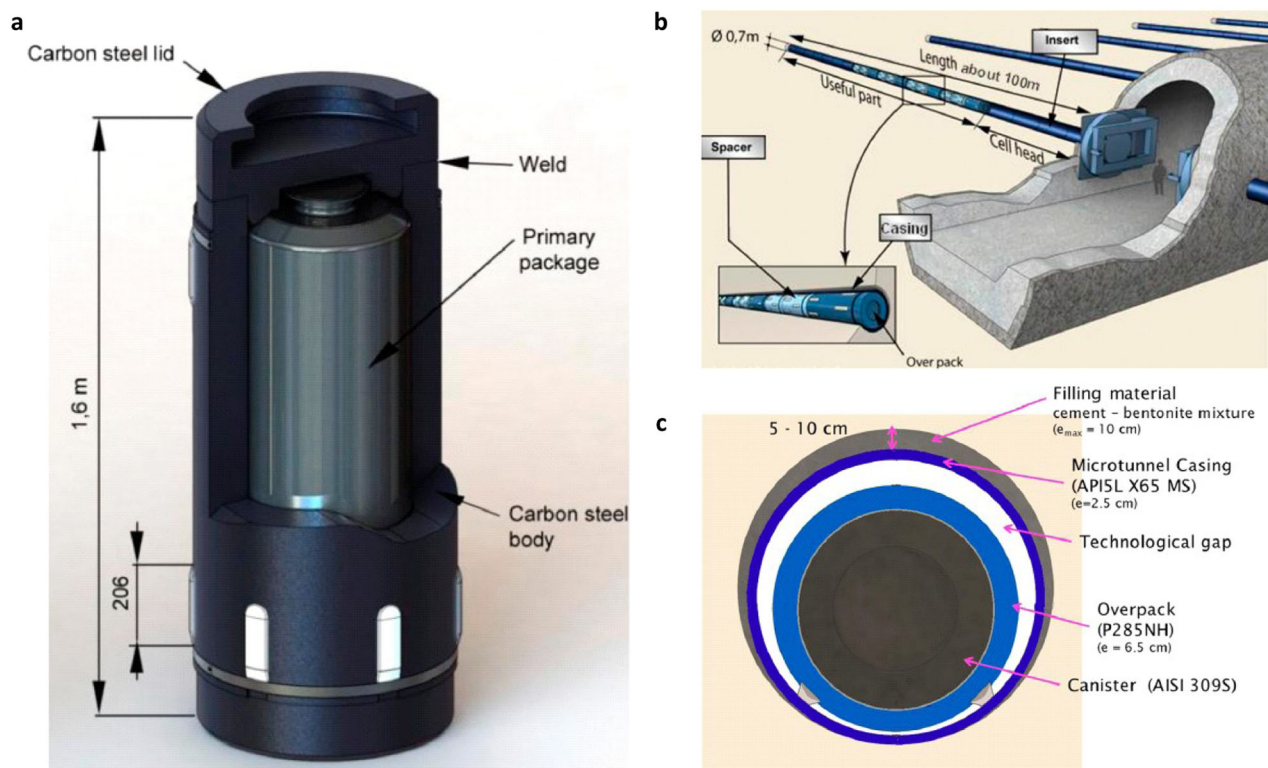
Fig. 2   Schematic illustration of French HLW disposal concept. a A typical stainless-steel primary canister containing vitrified high-level waste in the carbon steel overpack. **b** Horizontal micro-tunnels for the storage of waste package. **c** Cross-section of a typical waste package. Images take from Crusset et al.[12] with permission, copyright Taylor & Francis Ltd, 2017.

a safety standpoint. Therefore, CS is a suitable pilot material to study the nearfield corrosion interactions. However, it should be noted that CS will be passive like CRAs in alkaline environments and exhibit a low corrosion rate in anoxic neutral environments. It is well established that the corrosion mechanism, rate, and product of CS strongly depend on the presence of oxygen in the environment[27,28]. For example, when aggressive species such as Cl^- ions are below the threshold concentration, CS is likely to experience general corrosion under the anoxic condition dominant at the French and Belgian repository sites[20]. However, localized corrosion could still occur when CS is passivated by the increased pH during corrosion and the concentration of Cl^- ions exceeds the threshold[29]. The occurrence of localized corrosion will be further complicated by the presence of a radiation field, which creates various oxidizing species in nearfield environments[30]. Compared to anoxic conditions, localized corrosion of CS can occur more readily in oxic environments due to the smaller difference between the breakdown potential and corrosion potential, assuming other environmental conditions (e.g., solution composition, pH, and temperature) are similar. The corrosion rate of CS essentially depends on temperature, pH, and solution chemistry. However, in neutral solutions, a higher corrosion rate is generally expected for CS exposed to an oxic environment compared to the anoxic one, and the rate monotonically scales with the oxygen concentration to a specific range[31]. Moreover, in an anoxic repository environment, the dominant corrosion product is Fe_3O_4, while $Fe(OH)_3$ will be the primary corrosion product in an oxic environment[28,31] although Fe_3O_4 can also form and is often associated with crevice corrosion[32]. The presence of CO_2 further complicates the situation because siderite ($FeCO_3$) and $Fe_2(OH)_2CO_3$ could also form[33]. The different corrosion products of CS (primarily Fe(III) and Fe(II) species) derived from the different redox environments have a substantial effect on the corrosion of nuclear waste glass present in the close proximity, which will be discussed in Section "Glass and steel corrosion products". Owing to these differences, the impact of CS corrosion on the degradation of adjacent materials will be different for the oxic and anoxic repository environments. Hence, although other environmental parameters (e.g., temperature, solution chemistry, radiation, etc.) also contribute to the nearfield corrosion interaction between the materials covered in this review, we subdivide this section into two parts on the basis of the oxic and anoxic environments, which correspond to the proposed repository conditions for the U.S. and other countries, respectively.

Oxic environment
One of the earliest studies of the interaction of CS and glass was by McVay et al., who reported a synergistic corrosion interaction between PNL 76–68 nuclear waste glass and CS[34]. The authors immersed the two materials in the same aerated solution (deionized (DI) water, tuff, or basalt groundwater) at 90 °C without placing them in contact with each other. They found that the corrosion rate of both materials was enhanced due to their mutual interactions. This synergistic effect was explained by the precipitation of iron-silicate corrosion products, which effectively removed Fe^{3+} and silicates from the solution and thus prevented saturation of the solution with glass or CS corrosion products. The suppressed solution concentration subsequently drove the continuous degradation of both the glass and steel. This process has been recognized as one of the major mechanisms regarding the acceleration effect of metallic Fe on glass corrosion and has been validated by numerous studies as will be discussed below. However, in many scenarios, the glass will be in direct contact with a SS, not CS, canister. Furthermore, the direct contact of the materials may alter the resulting corrosion mechanism.
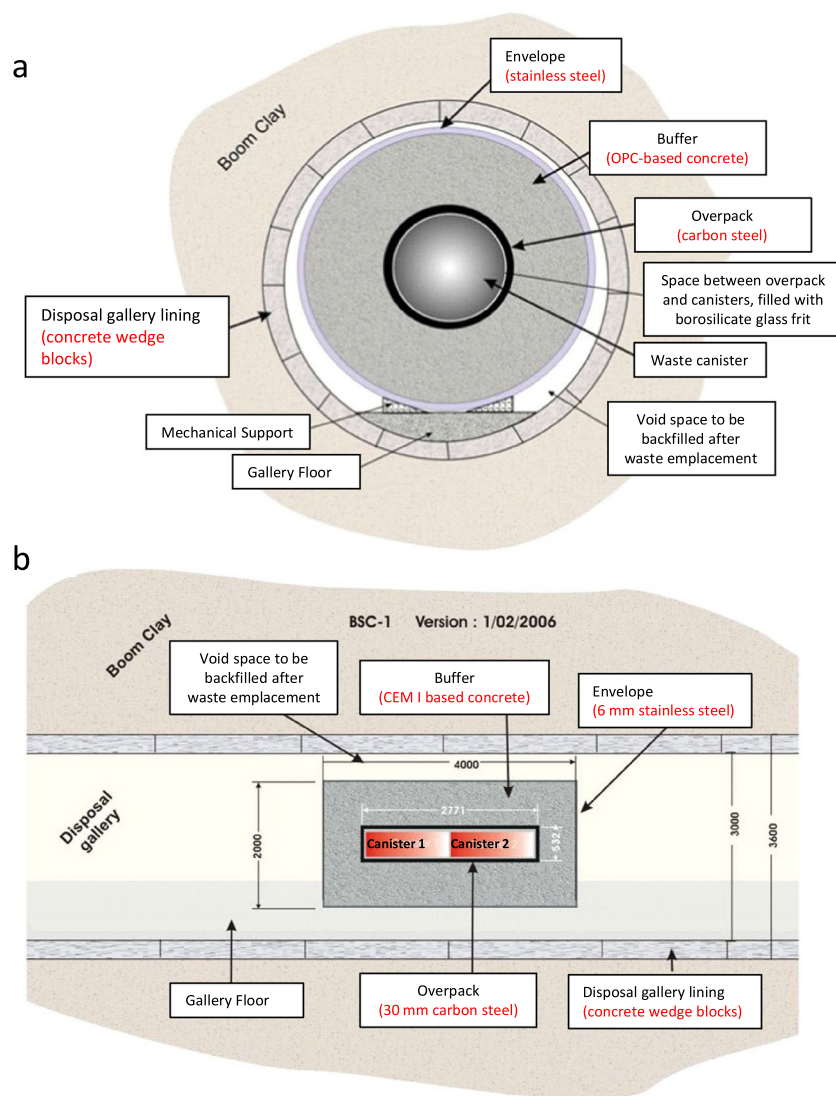
Fig. 3 Schematic diagram of Belgian supercontainer disposal concept. a Cross-section and **b** longitudinal section of the super-container. Figures adapted from Kursten et al.[20] with permission from Taylor & Francis Ltd, copyright Institute of Materials, Minerals and Mining, 2011.

Anoxic environment

De Combarieu et al. used a carefully-designed glass-iron-clay stack of materials in contact, thereby simulating the multi-barrier system in the French repository, to study the corrosion interactions between these materials[26]. A schematic illustration of the experimental setup is given in Fig. 4a, b. A thin Fe foil was directly contacted with a disk of SON68 glass, a non-radioactive surrogate for French nuclear waste glass, and corroded in contact with a water saturated with Callovo-Oxfordian Claystone at 90 °C for up to 18 months. After 10 months of exposure, the Fe foil was completely corroded, leading to the formation of a dense product layer (DPL) primarily consisting of Fe_3O_4, $FeCO_3$, and Fe-rich phyllosilicates (Fig. 4c). The corrosion of glass led to the development of a gel layer, the thickness of which continuously increased over time. Only 57% of Si was retained in the gel, implying a low protectiveness of this layer. A thin layer enriched in Ca, Ln, Mo, and P exists between the DPL and the gel, a secondary precipitates layer (SPL), which resulted from the precipitation of glass corrosion products. The presence of Fe in the gel, SPL, and DPL is clear evidence of Fe/glass corrosion interaction. These coupled interactions continuously maintained the glass dissolution rate at a level similar to the initial rate throughout the 18-month testing period, with only a slight tendency to slow down. In

addition to the mechanism involving the precipitation of iron-silicates, the authors suggested that Fe corrosion may constantly consume silicates in the solution, thereby suppressing the recondensation of dissolved silicates that might close the pores within the gel layer[35,36]. Thus, the resulting gel with open porosity could not act as an effective barrier for the mass transport of reactive species[37–39].

Burger et al.[40] applied a similar approach as De Combarieu et al., in which a glass-iron-clay stack was corroded in deaerated flowing synthetic clayey solution in equilibrium with the Callovo-Oxfordian claystone at 50 °C for up to 2 years. Instead of the iron foil used by De Combarieu et al., drilled iron disks filled with iron powders were employed by Burger et al. to enable water circulation through different layers of materials. After exposure, a complex alteration layer developed on the glass surface, with an inner porous gel layer covered by an outer layer consisting of iron-silicates (Fig. 5). The precipitation of the iron-silicate layer on the glass surface was found to depend on the distance to the iron powder; the corrosion of glass in the immediate vicinity of iron was apparently enhanced, as evidenced by the increased gel layer thickness in this region. The acceleration effect of Fe was primarily ascribed to the precipitation of iron-silicates and the deteriorated protectiveness of the gel layer. It is worth noting that iron-silicates
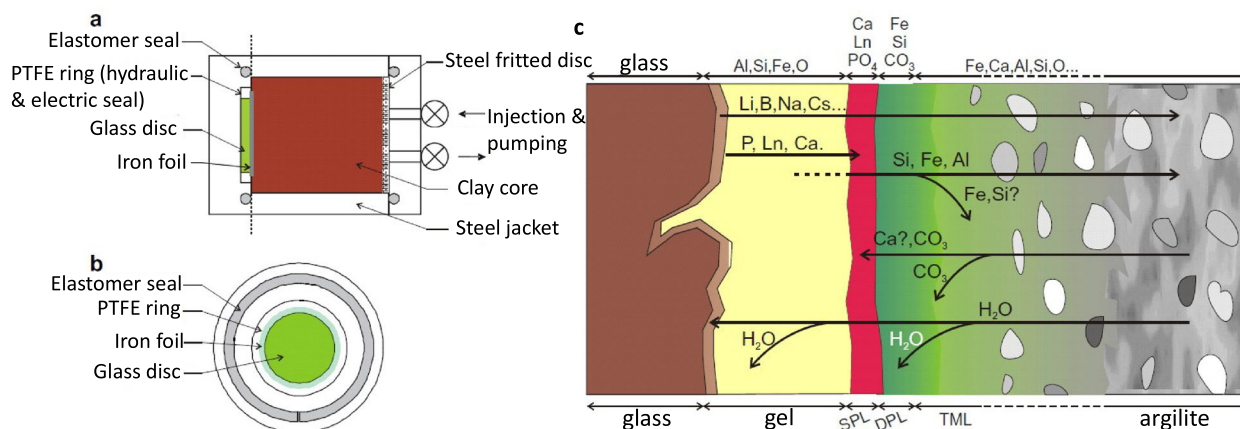
Fig. 4 Schematic illustration of corrosion interactions between iron and SON68 glass. a Side and **b** Top view of the experimental setup. **c** The structure and chemistry of different alteration layers after exposure. SPL: secondary precipitates layer. DPL: dense product layer. TML: transformed matrix layer (from clay). Adapted from De Combarieu et al.[26] with permission, copyright Elsevier, 2011.

were not only identified on the surface of the gel layer, but also within the gel. The authors hypothesized that Fe cations may have diffused into the gel from the metal/glass interface, reacted with silicates in the nanopores of the gel, and subsequently precipitated as nanosized iron-silicates. However, it is not clear how the incorporated Fe impacts the protectiveness of the gel, and further study is required.

A follow-up study was conducted by Michelin et al.[41], who performed a similar short-term study (756 days) using the glass-iron-clay stack like Burger et al.[40], and compared the result to an archeological analog exposed for 450 years. The archeological analog was a phase-separated calcium silicate glass with metallic iron inclusions embedded within the matrix. This material has been exposed to an anoxic clay environment similar to the French repository condition, so the underlying corrosion mechanism may be comparable to the case of nuclear waste glass. This hypothesis was supported by the notion that the infield long-term corroded glass exhibited an alteration layer structure similar to the short-term one formed in laboratory experiment under controlled conditions. As shown in Fig. 6, the pristine archeological glass substrate was covered by an inner alteration layer and an outer iron-silicate layer. After comparing glasses corroded with and without iron in the close proximity, it was concluded that the presence of iron accelerated the corrosion of glass during both long- and short-term exposures. Thus, the authors suggested that the iron-glass corrosion interactions observed in the short-term study could be extrapolated to predict longer term behavior and that the adverse effect of iron on glass corrosion could be sustainable over a longer timescale. Consistent with De Combarieu et al.[26] and Burger et al.[40], Michelin et al.[41]. also identified the incorporation of Fe within the gel layer. Several potential effects of iron incorporation were proposed by the authors: (1) Iron cations, probably Fe^{3+}, could be integrated into the gel as a network former. (2) Iron cations, likely Fe^{2+}, could also serve as a network modifier, which could depolymerize the silica network. (3) These cations may act as precursors for iron-silicate precipitation within the pore water of the gel. The oxidation state of iron revealed by scanning transmission X-ray microscopy was in support of hypothesis 3, so the authors believe that the small-scale precipitation phenomena may have a similar effect as the precipitation of iron-silicates in the bulk solution. Although this precipitation might potentially clog the porosity of the gel and slow down glass corrosion, it was not observed experimentally in this study. Based on a recent work showing that ions with large ionic radius such as K^+ or Cs^+ could significantly impact water content and mobility within the pores of the gel[42], it can be

hypothesized that incorporation of high amounts of Fe into the gel will impact the long-term behavior of the glass.

The same group of authors performed a separate study by corroding an iron foil sandwiched between two slides of synthetic representatives of an archaeological glass in deaerated Callovo-Oxfordian clay-saturated groundwater at 50 °C for up to 20 months[14]. As expected, the presence of metallic iron continuously enhanced glass corrosion, which was attributed to the iron-silicate precipitation mechanism. The resulting alteration layer formed on the simulated glass exhibited a similar structure to what is shown in Fig. 6. Some interesting observations should be noted in this study: (1) The iron foil was deeply corroded at the edges of the iron/glass contact area, while the corrosion was less evident in the center. (2) For glass corroded near the iron foil, the thickness of the alteration layer at the edge was significantly higher than that of the center. A similar phenomenon was observed for the glass corroded without iron, but it was less evident. This finding is consistent with the work by Dillmann et al.[43] (Fig. 7), which will be reviewed below. (3) The precipitation of iron-silicate slowed down when the iron foil was separated from the glass slide due to corrosion, suggesting that the proximity of these two materials is required to maintain the precipitation. A similar conclusion was also obtained by Reiser et al.[44] (4) The influence of iron seems to be highly localized. Although it was not discussed by the authors, these phenomena could be due to the crevice corrosion of iron, which is a critical mechanism driving the metal/glass corrosion interaction identified by Guo et al.[45] as described below. Indeed, the general corrosion of iron is likely dominant in the study by Michelin et al., especially at the beginning of the exposure. As the corrosion of glass and iron proceeded, the solution pH increased, which may have led to the passivation and subsequent crevice corrosion of the iron. Whether crevice corrosion can occur in an anoxic condition depends primarily on the environmental details, including but not limited to temperature, pH, and concentration of Cl^- ions[29]. Studies showed that crevice corrosion of CS can initiate when the concentration of Cl^- exceeds a threshold of 0.12–1.2 mM in an anoxic and alkaline environment in a temperature range of 65–95 °C[29]. The Callovo-Oxfordian clay-saturated groundwater used by Dillmann et al.[43] contained ~40 mM of Cl^- and the solution pH might have increased to a level sufficient to passivate the CS during corrosion, therefore, the occurrence of crevice corrosion under the testing condition is possible. However, when the gap of the crevice gradually opened due to the dissolution of both materials, the mass transport limitation within the crevice was eliminated, which subsequently reduced the corrosion rate of the passivated iron and resulted in the reduced precipitation of
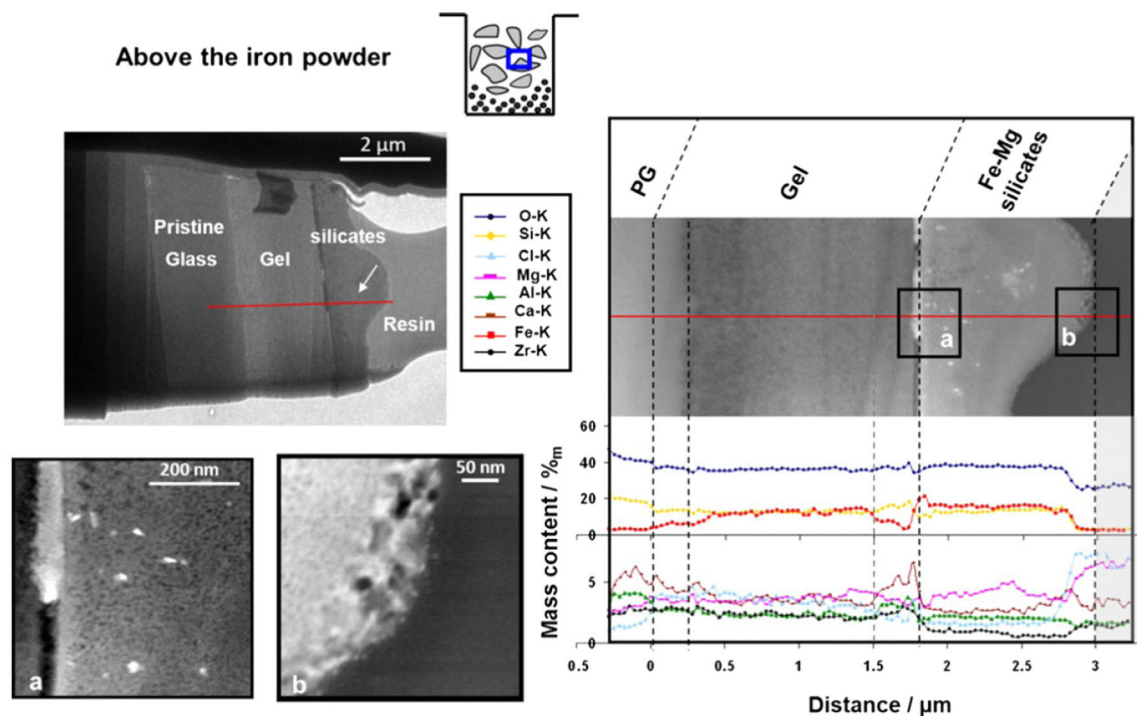
Fig. 5 SEM and TEM images and the corresponding EDS line profiles of the iron-glass interface. PG stands for pristine glass. Reproduced from Burger et al.[40] with permission, copyright Elsevier, 2013.

iron-silicates. This hypothesis needs to be validated by further studies.

It must be emphasized that, although the use of CS enables the observation of metal-glass interactions in a relatively short period due to its low corrosion resistance, the corrosion mechanism involved may not necessarily apply to other material systems. As above mentioned, CS undergoes general corrosion in acidic and neutral solutions, so the corrosion processes involved are distinctly different from the localized corrosion dominant on most CRAs and the interactions with glass might be different. Therefore, it is important to examine the corrosion interactions between glass and CRAs, particularly SS, which is the candidate canister material planned by many countries, including U.S. and France.

Glass and corrosion-resistant alloys

Some metals (e.g., Al, Ti, Ni, and Cr) are resistant to aqueous corrosion owing to the spontaneous formation of a thin and dense film called a passive film on their surfaces. Inspired by the natural protectiveness of such surface film, metallurgists have developed numerous CRAs that possess superior protectiveness against corrosion. The most broadly used CRAs to date are those based on Fe–Cr (e.g., SS) and Ni-Cr (e.g., Alloy 22), both relying on the formation of a robust Cr-rich oxide passive film on the alloys surface. Such CRAs are highly resistant to general corrosion. However, in a sufficiently aggressive environment, the passive film could breakdown and result in the locally accelerated dissolution of the alloy substrate in the form of pits on boldly exposed surfaces or crevices at shielded regions. The localized corrosion of metals and alloys have been extensively reviewed elsewhere[23,24,46]. It should be noted that this section only discusses studies performed in oxic conditions due to the lack of relevant studies in anoxic environments. Evidently, more attention should be paid to investigate the corrosion interactions between glass and CRAs, such as SS under anoxic conditions.

CRAs are intentionally designed with a low rate of general corrosion, so it is challenging to design experiments on a short

laboratory timescale to successfully reveal their influence on glass corrosion. For example, Burns et al. examined the corrosion of Savannah River Plant (SRP) simulated nuclear waste glass in the presence of a series of metals including CRAs: A516 low CS, SS304, SS409, SS430, alloy E-brite, TiCode-12, and Inconel 600[47]. For each experimental group, one monolithic glass coupon was placed adjacent to one metal/alloy specimen and corroded in DI water or simulated basaltic groundwater at 90 °C for 28 days. As expected, A516 CS strongly increased the corrosion rate of glass. However, the other alloys only slightly increased glass corrosion during the testing period. The absence of strong corrosion interaction between these CRAs and glass might be associated with the mild solution chemistry employed in this study. DI water is an extremely mild environment for CRAs and, although ~150 ppm of aggressive Cl⁻ is typically present in basaltic water, such a concentration is less than the maximum limits (hundreds of ppm) recommended for exposure of SS[48]. If it could be guaranteed that the exposure environment would remain nonaggressive, then corrosion of these CRAs and interactions with glass might not be a problem. However, in more aggressive environments, the CRAs might undergo localized corrosion and the interactions with glass might be much different under those conditions.

Another effort was made by Barkatt et al., who examined the corrosion interactions between SRL TDS-131 glass and SS304L, both of which were in form of powders with different metal/glass surface area ratios[49]. A leaching study was performed by immersing the glass with/without the presence of SS304L in DI water at 70 °C for a period up to 120 days. SS did not significantly affect the glass corrosion, particularly when the surface area of SS was smaller or nearly equal to that of glass. When the surface area of SS was ten times larger than that of the glass, a transient suppression effect was observed on the leaching rate of Ca and Sr, whereas the rest of the elements were not affected. The authors suggested that the difference was associated with the chemisorption of the dissolved Ca and Sr species on the large surface of the SS powders. However, it is not clear why the glass corrosion was inhibited in the early stage of the exposure because the sorption
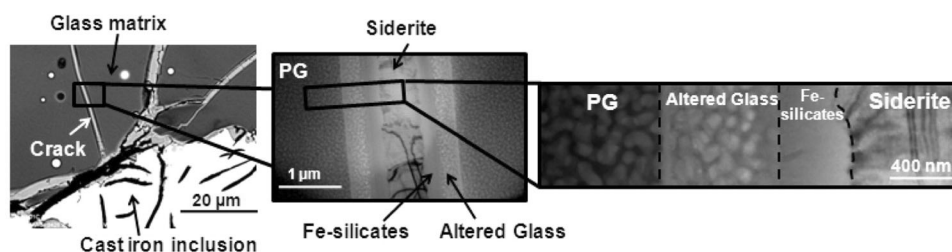
Fig. 6 Microstructure of the alteration products formed on the surface of archeological glass sample. Reproduced from Michelin et al.[41] with permission, copyright American Chemical Society, 2013.
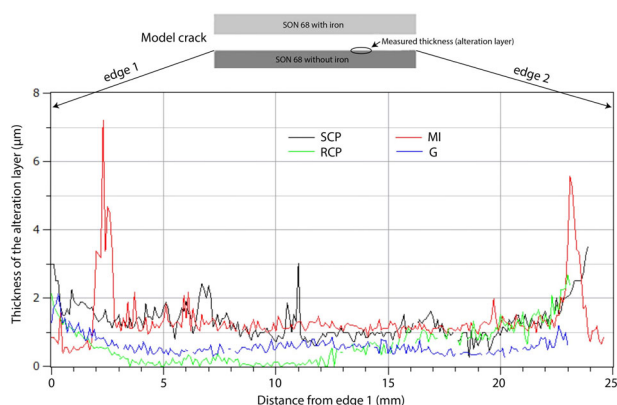
Fig. 7 Thickness profiles of the alteration layer formed on glass corroded with: synthetic corrosion products (SCP), metallic iron (MI), representative corrosion products (RCP), or glass without other materials (G). Reproduced from Dillmann et al.[43] with permission, copyright Elsevier, 2016.

effect typically increases glass corrosion. Nonetheless, the weak corrosion interactions between SS and glass observed in this study, again, may be due to the absence of aggressive anions (e.g., Cl^- ions) in the leaching solution. Without these ions, the dominant corrosion mechanism of SS was likely passive dissolution, which is typically many orders of magnitude slower than the localized corrosion. If aggressive anions were present to break down the passivity of the SS, the higher corrosion rate of SS could subsequently influence the corrosion of the glass nearby. Although the SS powders were in direct contact, to an extent depending on the volume ratio of metal and glass powders, crevice corrosion probably did not occur on a large scale, not only due to the lack of aggressive anions, but also the absence of confined geometry necessary to enrich aggressive metal cations. Therefore, powdered samples may not be suitable for the assessment of corrosion interaction between glass and CRAs.

The following year, Woodland et al. embarked on a 5-year-long project to explore the potential corrosion interactions between SRL U Glass (SRL 165 black frit doped with Cs, Sr, and U) and SS304L[50,51]. A drip test approach was applied to simulate the actual repository environment in the U.S. Yucca Mountain project. The experimental apparatus is provided in Fig. 8. In brief, a glass specimen was enclosed in an artificially perforated holder made from SS304L to form a waste package assemblage (WPA). The WPA was contained in a sealed testing vessel also made from SS304L. A constant volume of J-13 well water (water from a well near Yucca Mountain) was allowed to drip to the surface of the WPA at a predesignated interval. The composition of the leaching solution was monitored throughout the 5-year testing period, while the characterization of solid-state specimens was performed for up to 1 year.

For glasses corroded without the SS holder, a minimum amount of elemental release was observed compared to other

experimental groups. Progressive precipitation of aluminosilicates, calcite, and gypsum minerals was identified on the glass surface. When the glass was corroded in the presence of SS, an approximately two-fold increase in the release rate of Li, B, and U was observed. When the top and bottom surfaces of the glass remained wet throughout the testing period, a ten-fold increase in the leaching rate was observed[50]. Solid-state characterization revealed a well-defined boundary between the contact and noncontact regions of the SS and glass. Similar to glass corroded without SS, an alteration layer formed on the surface of the glass corroded in the presence of SS and incrementally coarsened over time. This layer was Si-rich and consisted of Fe, Ca, Mg, Na, Mn, Ni. The composition is similar to Fe-smectite and amorphous hisingerite. $CaSO_4$, Fe-oxide/hydroxide[51], brookite, and davidite $(Fe,Ce,U)_2(Ti, Fe)_5O_{12}$/thorutite $(Th, U, Ca)Ti_2O_6$[52] were embedded within the cracks between the flakes of the alteration layer. The authors suggested that this discontinuous alteration layer is not a reliable barrier for the transport of reactive species. Due to the presence of a network of cracks, this layer may gradually exfoliate from the surface, exposing the pristine glass to the electrolyte, thus resulting in accelerated corrosion of the glass. Interestingly, zeolite was identified on the glass surface after 26 weeks[52], but it is not clear whether a similar mineral was observed on glass corroded without SS. Meanwhile, a film enriched in Si, Mn, Cr, and Fe gradually developed on both the contact and noncontact surface of the SS. SS also acted as sites for the precipitation of multiple secondary phases. These findings are consistent with a later study by Guo et al.[45].

It is worth noting that the degree of corrosion was greater on the bottom surface of the glass than on the top. This could be due to the different wetness in the two locations, or the different size of the gap between the glass and SS holder caused by gravity. Although the latter implies the occurrence of SS crevice corrosion, the authors suggested no localized damage was visible on the SS after the exposure. It is possible that the drip test was not aggressive enough to trigger crevice corrosion. As shown by the authors, the leaching rate of glass under the drip test condition was 2–15 times lower than that of the full immersion test. However, the interpretation based on the nonaggressiveness of the environment seems to be less likely because numerous studies have shown that localized corrosion of SS can occur under similar atmospheric conditions at a lower temperature[46,53–55]. Therefore, an alternative and more reasonable explanation may be that the geometry of the experimental setup in this study does not favor the occurrence of crevice corrosion. As suggested by the authors, there was no close contact between the SS and glass during the experiment. Additionally, the contact area of the SS and glass appears to be too small owing to the presence of multiple holes intentionally designed to simulate the post-perforation scenario of the SS canister. As a consequence, without a sufficiently large contact area and a tight gap, the accumulation of aggressive species, such as metal cations and Cl^- ions may not occur[24,56], so crevice corrosion might not be initiated under the testing conditions.
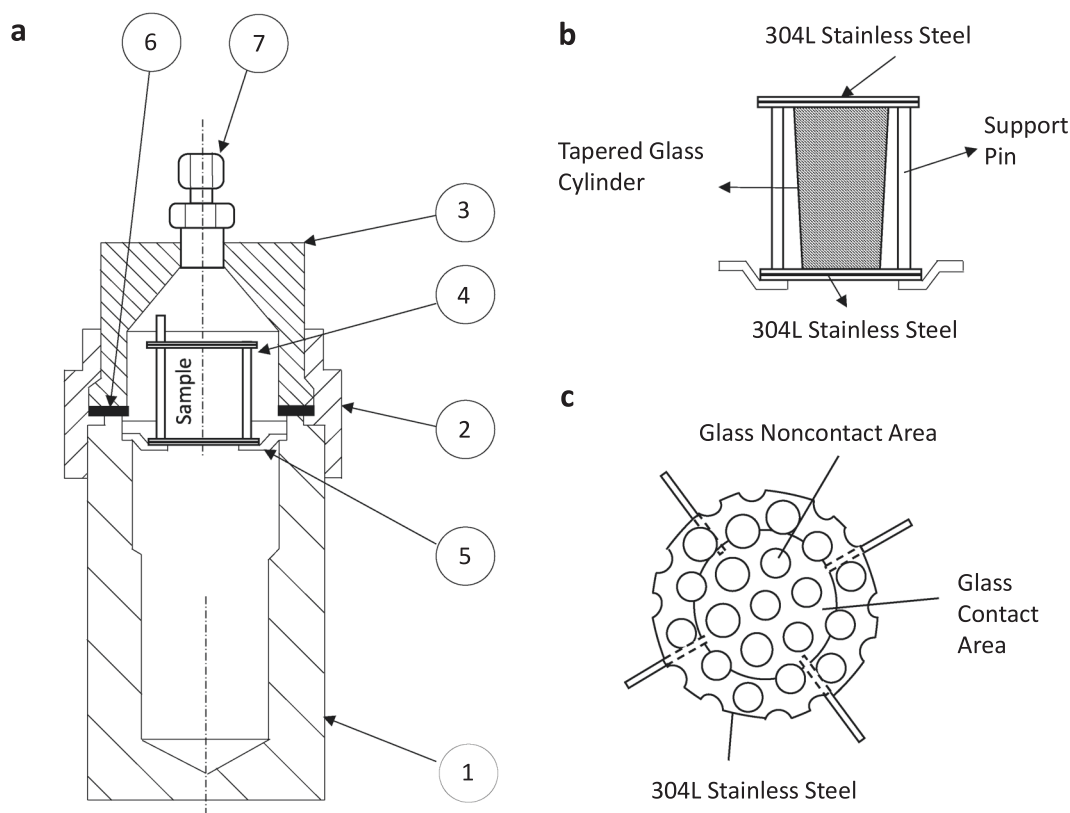
Fig. 8 Schematic illustrations of the experimental apparatus. a Test vessel. 1. Body. 2. Nut. 3. Cap. 4. Retainer top. 5. Retainer bottom. 6. Ethylene propylene gasket. 7. Swagelok fitting. **b** Side and **c** top views of the SS/glass assembly. Reproduced from Bates et al.[50] with permission, copyright Materials Research Society, 1990.

In recent studies, a mechanism of nearfield interaction based on metal crevice corrosion was disclosed by Guo et al., as schematically illustrated in Fig. 9[30,45,57]. The authors corroded international simple glass (ISG) or soda lime silica glass (SLSG) in close proximity to SS316, Alloy 625, or Alloy G30 in 0.6 M NaCl solution or DI water at 90 °C for 14 or 30 days. Specimens of different materials were pressed against each other to form a crevice between them, so the mass transport within the crevice space was limited, which is critical for the initiation of metal crevice corrosion. After the predesignated exposure time, crevice corrosion characteristics were observed on the surface of both the alloys and glasses, where the corrosion damage was localized at the boundary of the alloy/glass contact area (crevice mouth). The damage was attributed to the enriched metal cations and protons generated by the anodic dissolution of the alloys. In turn, the attack by these locally accumulated cations and protons preferentially enhanced the thickness of the gel layer at the crevice mouth, which was also observed by Michelin et al.[14] and Dillmann et al.[43] (Fig. 7). Additionally, the structure and chemistry of the gel in this area were both altered. Precipitation of an Fe- and Si-rich surface film was identified on the surface of the SS, which may have played a similar role as the iron-silicate precipitation retarding the solution saturation with respect to silica. Apart from the influence introduced by the anodic dissolution, the cathodic reactions occurred on the SS also have a substantial effect on glass corrosion. It was found that the oxygen reduction reaction on the SS surface enhanced the alkalinity on the cathode of the SS and facilitated the precipitation of Si-bearing secondary phase minerals, including zeolites and iron-silicates. Extensive studies have shown that these Si-bearing minerals can enhance glass corrosion by disrupting the steady-state corrosion of glass and triggering the Stage III glass corrosion regime[58]. While the corrosion of glass was clearly enhanced by SS

in both DI water and NaCl solution, the effect of glass on the corrosion of SS depended on the solution chemistry[57]. In NaCl solution, the glass corrosion products, primarily silicates, inhibited the corrosion of SS, owing to the suppression of the SS passive film breakdown. In contrast, SS corrosion was enhanced by the corrosion products of glass in DI water. This is likely associated with the presence of Al^{3+} ions generated from glass corrosion, which might have increased the breakdown frequency of the SS passive film in the mild environment.

The mechanism described by Guo et al.[45] applies to the scenario when the SS canister fails and the underground water comes in contact with both the SS and nuclear waste glass. Due to the presence of the robust passive film, SS is most likely breached by localized corrosion from the outside, while the majority of the canister will remain intact or less corroded. As corrosion proceeds, the corrosion products derived from both the SS canister and glass may gradually accumulate at the interface of the two materials. Part of the corrosion products may transport to the nearfield environment given the aggressive condition (high concentration of H^+ and Cl^- ions) existing at the interface owing to the localized corrosion of SS. The precipitation of corrosion products or secondary phases at the glass/alloy interface could further restrict the mass transport between the crevice and the bulk solution, as well as enhance the ohmic potential drop (between the anode and cathode), both of which might subsequently accelerate the crevice corrosion of SS and enhance the nearfield corrosion interaction. It is expected that the gap of the crevice between the SS and glass will become enlarged as both materials are consumed over time, thus reducing the rate of SS crevice corrosion. However, crevice corrosion can be further activated at other locations where the glass and SS are in close proximity (not necessarily in direct contact). It is well established that the rate of metal crevice corrosion is proportional to a scaling
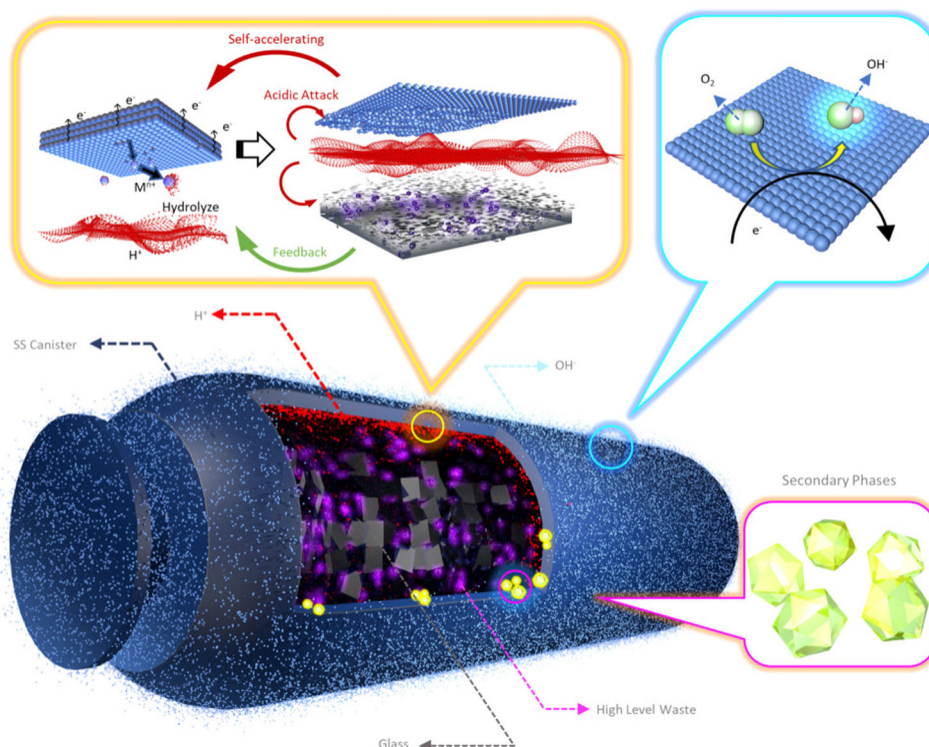
Fig. 9   Schematic illustration of interactive corrosion behavior between SS canister and nuclear waste glass[45]. The anodic dissolution of SS creates a high concentration of metal cations (M^{n+}) on the interior surface of the SS canister. These metal cations hydrolyze, acidify the local solution, and attack the adjacent nuclear waste glass. In addition, the cathodic reaction occurs on the exterior surface of the SS canister, enhancing the alkalinity in the surrounding environment and subsequently assisting the precipitation of secondary phase minerals that could adversely impact glass corrosion.

factor dictated by the ratio of the shielded area of metals to the crevice gap size[24]. Consider the large contact area between the glass and SS canister and the much smaller crevice gap, crevice corrosion of SS could easily initiate and propagate to a great extent. Although the study by Guo et al.[45] was performed in an oxic condition, the mechanism might also apply to an anoxic environment, particularly when a radiation field is present[30]. Further studies are required to assess this situation.

Glass and steel corrosion products

Apart from metals and alloys, various steel corrosion products can also accelerate the corrosion of glass. Studies showed that these interactions depend on the aeration condition of solution, probably via changes in the redox potential of the environment. For example, Inagaki et al. corroded powdered simulated waste glass in the presence of Fe_3O_4, under both oxic and anoxic conditions (Ar + 5%H_2)[59]. In most cases, Fe_3O_4 is the dominant corrosion product of iron in anoxic conditions[28,31]. However, Fe_3O_4 can actually form in an oxic environment when crevice corrosion is involved[32]. This is expected because oxygen within the crevice is often depleted by the cathodic reaction, leading to a local anoxic environment that could exist until the mass transport limitation is eliminated. Regardless of this argument, Inagaki et al.[59] revealed an acceleration effect of Fe_3O_4 on glass corroded under both oxic and anoxic conditions, but the effect was less evident under anoxic conditions. Although it was not discussed by the authors, it is possible that the Fe^{2+} species in the Fe_3O_4 was further oxidized to Fe^{3+} in the oxic environment, leading to an enhanced surface area with higher Si sorption capacity[60]. However, this hypothesis needs to be verified by further studies.

Kim et al. reported a similar acceleration effect of $Fe(OH)_3$ on the corrosion of simulated borosilicate waste glass under both oxic (aerated DI water) and anoxic conditions (Ar-purged DI water)[61]. However, the authors suggested that the effect of $Fe(OH)_3$ is stronger under anoxic conditions than oxic conditions. Interestingly, when the $Fe(OH)_3$ powders were absent, the glass corroded several times faster under oxic condition than anoxic condition. The authors ascribed the different behaviors of $Fe(OH)_3$ in the two environments to the presence of $Fe(II)$ impurities accompanying the $Fe(OH)_3$ powders. However, no detailed mechanism was provided, so it is not clear how the small amount of $Fe(II)$ impurities had such an effect. In addition, the root cause of the contradictory results obtained by Inagaki et al. and Kim et al. also remains unclear, although it might be associated with the difference in materials, temperature, and the purging gas used in the two studies. Therefore, there is an obvious scientific gap regarding how aeration condition influences the interactions between glass and steel corrosion products. The lack of data available for oxic conditions made it difficult for comprehensive comparison between oxic and anoxic conditions. Therefore, the following discussions of this section focus primarily on the corrosion interactions between glass and steel corrosion products in anoxic environments, with one exception for the study by Neill et al., which was conducted in an oxic condition[62].

Bart et al. reported the enhanced corrosion of Swedish and French model nuclear waste glass in the presence of Fe_3O_4 or the corrosion product of SS304 with varied surface area ratios in an anoxic environment[63]. An acceleration factor of 4–5 was identified for the synthetic Fe_3O_4 with a high effective surface area, indicating that the acceleration effect is associated with a sorption mechanism. The sorption of silicates to Fe_3O_4 is similar to what was reported by Werme et al.[64], who described that the sorption of silicates on Fe_3O_4 or $FeOOH$ accelerated the corrosion rate of glass. This short-term acceleration effect was eliminated when the sorption sites were completely occupied. With the help of the

surface complexation model, the sorption capacity of Si on various steel corrosion products (e.g., Fe_3O_4, $FeOOH$, Fe_2O_3, $FeCO_3$, and FeS) has been systematically studied by Philippini et al.[65], and Jordan et al.[60], which enables the estimation of the influence of different Fe-containing materials on glass corrosion. Notably, Bart et al. found that glass corrosion was enhanced more significantly in the presence of the actual corrosion product of SS304 than the synthetic Fe_3O_4[63]. The resulting corrosion rate did not slow down even after one year of exposure. This finding highlights the necessity of identifying the possible role of other corrosion products of SS304 than Fe_3O_4.

Efforts have also been made to correlate the short-term observed corrosion interactions to a longer timescale with the help of archaeological analogues. For this purpose, Michelin et al. investigate the corrosion interactions between archaeological glass and $FeCO_3$[14]. The authors synthesized glass representatives on the basis of an ancient archaeological glass artefact and corroded them in close proximity to $FeCO_3$ powders in deaerated groundwater at 50 °C for up to 20 months. Similar to other steel corrosion products, $FeCO_3$ was found to accelerate glass corrosion (by a factor of 5–10) primarily through the silicate sorption mechanism. This effect was limited by the sites of sorption, so the acceleration effect gradually decreased over time. In contrast to glass corroded without any other materials, no gel layer was identified on glass corroded with $FeCO_3$, suggesting that the glass hydrolysis rate may be strongly enhanced by $FeCO_3$.

Following the work by Michelin et al.[14], Dillmann et al.[43] used a similar approach to study the effect of the formation conditions and the age of various iron corrosion products on the degradation of SON68 glass. Assuming CS will be consumed by general corrosion under the actual anoxic repository condition, the corrosion products of CS may form primarily on the outside of the overpack or canister. After intense and long-lasting interaction with the backfill materials such as bentonite and backfill clay that will exist in the French repository, the steel corrosion products will likely be saturated with Si. Hence, a crucial question is whether the Si-saturated corrosion products will still accelerate glass corrosion similar to the fresh corrosion products broadly used in laboratory testing[43]. For each experimental group, two monolithic SON68 coupons were separated by PTFE threads to form a gap in between. Powders of the 450-year-old representative corrosion products (RCP) of iron, synthetic corrosion products (SCP), and metallic iron (MI), were inserted into the gaps formed by SON68 glass specimens and corroded in anoxic groundwater at 50 °C for 6 months. The acceleration effect of these materials on glass corrosion was ranked as MI > SCP > RCP. The authors suggested that the marginal effect of RCP may be associated with the low thermodynamic driving force, because the RCP may have been equilibrated with silicates in groundwater after 450 years of exposure before the excavation. It is worth noting that, although the CS overpack may transform into less reactive corrosion products after a long period, the encapsulated SS canister will be most likely breached by localized corrosion. Hence, the corrosion interactions between metallic SS, glass, and CS corrosion products should all be considered in the real-world scenario, which should be a topic of interest for future studies. Systematic characterization was performed to study the corroded specimens on multiple length scales. Both iron carbonates ($FeCO_3$, $Fe_2(OH)_2CO_3$) and iron-silicates (nontronite, greenalite $(Fe)_{2-3}Si_2O_5(OH)_4$) were identified in various locations, including the gaps between different materials and the surface of iron or iron corrosion products. For glass corroded with SCP and MI, the iron-silicates were even found inside the glass gel layer, which could adversely impact the protectiveness of the gel. In addition to iron-silicates, Schlegel et al. found that discrete powellite or lanthanide hydroxycarbonates can also precipitate within the gel layer[66]. In brief, Dillmann et al. demonstrated that the corrosion interactions between iron or iron corrosion products and glass strongly depends on the

nature of the iron source, which could lead to the development of different solution chemistry, precipitates, and gel layers with different structure and morphology. This study highlights the importance of quantifying the influence of metallic canister at different stages, because this effect may vary as the alloy transforms into states that are thermodynamically more stable. Assuming a general corrosion mechanism, a CS overpack may be perforated after thousands of years, so the corrosion products of CS should be thermodynamically stable, or at least the less stable forms should have converted into more stable forms. However, it should also be emphasized that if the CS overpack is breached by localized corrosion while the majority of the CS remains intact, the impact of Si-saturation on the corrosion products of CS and the subsequent influence on nearfield corrosion interaction may be different and should be studied further.

Similar to glass and metal/alloys, the interaction between glass and steel corrosion products also depends on the proximity of the two materials, although the mechanism involved may be different. Rébiscoul et al.[67] explored the interaction between SON68 glass and Fe_3O_4 with and without a diffusive barrier in between. In both cases, the corrosion rate of glass was enhanced by a factor of 4–5, which again was primarily attributed to the sorption or precipitation of silicates on Fe_3O_4. When the two materials were mixed homogenously, the glass dissolution rate slowed down slightly faster than when a diffusion barrier was present. Additionally, a gel layer formed on the surface of the corroded glass (Fig. 10, GM1), which contained Fe with the same valence state as Fe_3O_4, suggesting a mechanism of dissolution-diffusion-reprecipitation. In contrast, when the two materials were separated by a diffusion barrier, a porous gel layer absent of Fe developed on the glass surface (Fig. 10, GSM1). The retarded formation of a dense protective gel layer correlates with the delayed establishment of the residual rate, likely associated with the longer time required to saturate the sorption sites of Fe_3O_4. This finding validates a competition for silicates between the sorption on Fe_3O_4 and the recondensation on glass, whereas the sorption may be kinetically favorable. Submicron scale characterization revealed that the gel layer was covered by an additional layer of secondary phase consisting of a mixture of iron-silicates and phyllosilicates. The combined result suggests that the incorporation of Fe and precipitation of iron-silicates strongly depend on transport of reactive species, which varies with the distance and time required for dissolved Fe cations to reach the glass. Notably, Rébiscoul et al. summarized four major mechanisms that may be responsible for the interactions between glass and Fe_3O_4: (i) sorption of Si on the surface of Fe_3O_4, (ii) precipitation of Fe/Mg-silicates, (iii) precipitation of SiO_2 on the surface of Fe_3O_4, (iv) incorporation of Fe within the glass gel layer. The relative importance of these mechanisms is not yet clear and seems to be environment dependent. In particular, when the sorption sites on Fe_3O_4 are saturated by Si, the acceleration effect on glass corrosion should decrease, which further highlights the importance of studying the corrosion interactions between glass and Fe_3O_4 completely saturated and equilibrated with nearfield materials.

The presence of surface defects on glass also plays an important role in the nearfield corrosion interactions. An interesting phenomenon was observed by Neill et al.[62], who corroded monolithic ISG in solutions pre-saturated with $^{29}SiO_2$ in a neutral oxic environment for 70 days, after which Fe_3O_4 powder was added to the leaching solution. For each ISG sample, only one of the six surfaces was abraded to eliminate surface defects while the other surfaces were left in the as-cut condition. Glass alteration following the addition of Fe_3O_4 powder proceeded much faster on surfaces having microcracks from cutting than on the treated surfaces. The authors suggested that Fe could act effectively at the defect areas, which possess distinct local chemical environments such as an increased diffusion constant of ions in the cracks and the enhanced alkalinity surrounding them. These defect-assisted
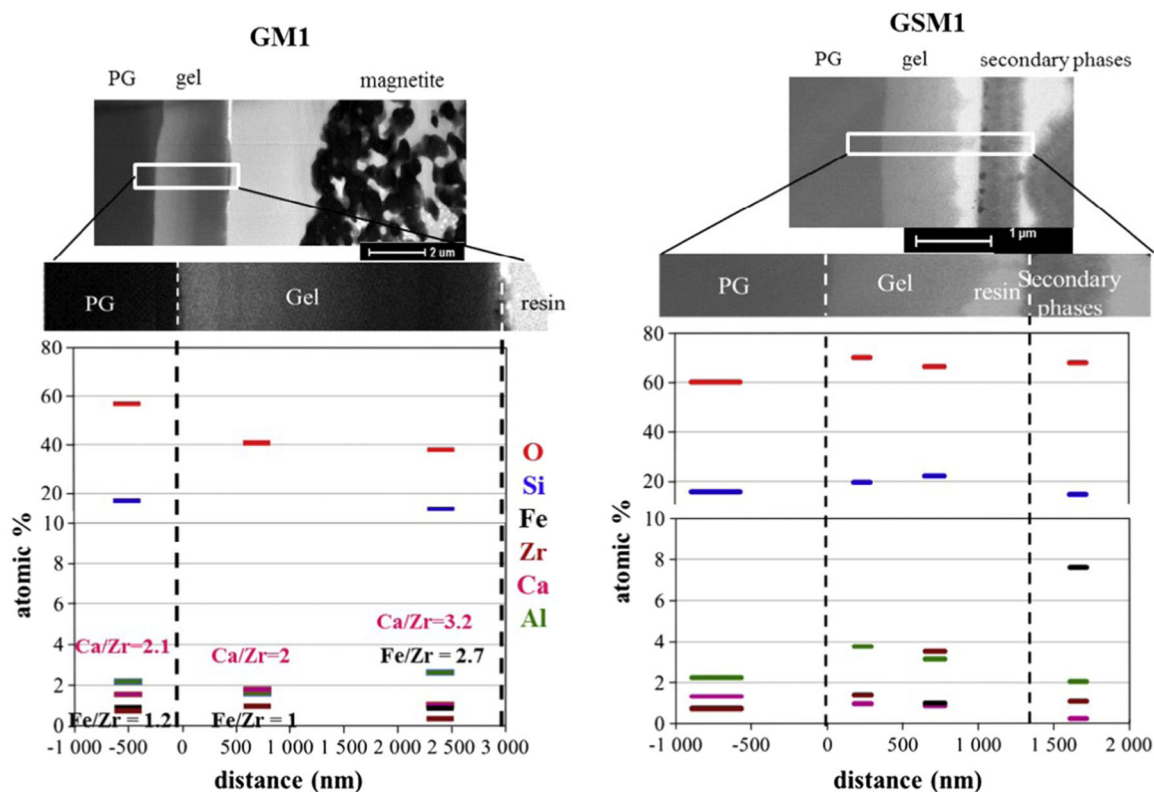
Fig. 10 STEM bright-field images of the interfaces between glass and Fe_3O_4 without (GM1) and with (GSM1) a diffusion barrier. PG: pristine glass. Reproduced from Rebiscoul et al.[67] with permission, copyright Elsevier 2015.

nearfield interactions should be taken into account because cracks are expected for the actual nuclear waste glass, primarily due to the cooling of the glass when cast into metallic canisters and the formation of mechanical fractures during the transport of the waste packages. This study highlights the role of nearfield corrosion interactions associated with coupled mechanical effects and chemical reactions. One of the important observations from this study is that the effect of accelerated glass corrosion lasted for a period exceeding 400 days, which was much longer than that of the previous studies described in this section. The Si-sorption mechanism cannot fully explain the much longer period of accelerated glass corrosion because the sorption sites of Fe_3O_4 were likely completely occupied, suggesting other mechanisms such as SiO_2 precipitation may have occurred. Since the experiment was conducted in an oxic environment, it is also possible that the Fe^{2+} species in the Fe_3O_4 were oxidized to Fe^{3+}, which resulted in an enhanced surface area with a higher Si sorption capacity[60]. A similar mechanism was proposed by Godon et al., who suggested that the long-term effect may be associated with the conversion of Fe_3O_4 to Fe_2O_3 or FeOOH in addition to the precipitation of Fe-silicates[68]. Since the occurrence of this long term effect is not consistently observed in the literature, it is thus crucial to understand under which conditions it will occur, and how it impacts the nearfield interaction on a timescale relevant to waste disposal.

Apart from experimental studies, efforts have also been made to model the corrosion interactions between glass and nearfield materials on the basis of the adsorption mechanism. For instance, Grambow et al. modeled glass corrosion in the presence of Fe_3O_4 using the GLASSOL model, which was coupled with the geochemical code PHREEQE[69]. The authors assumed that one monolayer of Si is adsorbed on the surface of Fe_3O_4 until saturation, after which the solution can be saturated with respect to Si. The simulated result agreed reasonably well with the experimental leaching data obtained for up to 1 year, validating the assumption that the initial acceleration of glass corrosion could be attributed to the sorption mechanism. However, the authors pointed out that the enhanced glass corrosion may still be possible after the sorption sites are completely occupied, because the multiple-layer sorption and precipitation of iron-silicates may occur subsequently.

Jollivet et al. simulated the corrosion of SON68 glass in the presence of simulated corrosion products (CP) of NS24 steel (63% Fe–23%Cr–13.5%Ni) or environmental materials (EM, e.g., bentonite, clay, granite, and smectite) using the LIXIVER 2 code[70]. The model was based on a similar first-order kinetic law used by Grambow et al.[69], which was coupled with the sorption and diffusion of Si. Five adjustable parameters were defined in this model to describe the properties of the glass and nearfield materials: two related to the kinetics of glass corrosion, including the total Si concentration at saturation (C^*) and the diffusion coefficient of Si in the pore water within the gel (D_g); one related to the adsorption capacity of CP (R_{ad}); two related to the properties of EM including the diffusion coefficient of Si in the pores of EM (D_p) and the Si distribution coefficient (K_d). The effect of CP was modeled by considering the sorption of Si until saturation (governed by R_{ad}), after which the CP was treated as inert with respect to glass corrosion. For glass corroded in the presence of EM, in addition to sorption, Si removal from EM was allowed by taking diffusion into account. With these five parameters, a good fit was obtained between the experimental data and the simulation, leading to some interesting findings. For example, a different K_d value could be obtained by fitting, which enables the comparison of the adsorption effect between different EM. Furthermore, by comparing the different fitted D_g values, it was found that the gel layer formed in the presence of CP, clay, and smectite was substantially less protective compared to the gel formed in the presence of DI water, bentonite, or

granite. It is worth noting that the K_d values obtained in this study did not match the actual values, suggesting other phenomena such as Si precipitation should be considered. This assumption was validated in a later study by Godon et al. who simulated the accelerated corrosion of SON68 glass in the presence of Fe_3O_4 using a geochemical code Hytec with a glass dissolution model (GRAAL[71,72]) while considering the sorption of silica on Fe_3O_4[68]. The simulation result was compared to data collected by experiments, which revealed that the sorption mechanism alone could not fully explain the high dissolution kinetics observed on the glass corroded with Fe_3O_4. A more reasonable agreement between the simulation and experiments was achieved after considering the precipitation of Fe-silicate minerals.

To summarize this section, the corrosion interactions between glass and steel corrosion products are governed by multiple factors, including the composition, formation condition, aging history, and proximity of the two materials, as well as the solution aeration condition and radiation field. Unlike the interactions between glass and metals/alloys involving both chemical and electrochemical reactions, the interactions between glass and most steel corrosion products are primarily physiochemical processes. Generally, at the early stage of interaction, the presence of steel corrosion products accelerates glass corrosion, predominately via a sorption mechanism that is determined by specific surface area of the materials and the mass transport. Once the sorption sites are fully occupied, other mechanisms may become dominant, including but not limited to the precipitation of SiO_2 and/or Fe-silicates, both of which might continuously drive the long-term interactions between glass and steel corrosion products.

Glass and aqueous Fe^{2+}/Fe^{3+} cations

Although extensive studies showed that glass corrosion can be enhanced by various solid-state materials, scarce literature exists regarding the effect of dissolved iron cations, which can be produced via both general and localized corrosion of most Fe-based alloys, as well as the dissolution of steel corrosion products. One important study came from Pan et al., who explored the corrosion of two model glasses (West Valley Demonstration Project (WVDP) glass and Defense Waste Processing Facility (DWPF) glass) in $FeCl_2$ and $FeCl_3$ solutions with varied concentrations (0.0025 and 0.25 M) and temperature (40, 70, and 90 °C) and a glass surface area to solution volume ratio of 2000 m^{-1} [73,74]. The iron chloride solutions used in this study can be considered reasonable surrogates for the possible internal waste package environment after perforation, particularly in the case of localized corrosion. Although Fe^{3+} has a low hydrolysis constant of ~2.2[75] and can easily form iron hydroxides in a bulk neutral solution, $FeCl_3$ and $FeCl_2$ salts are highly soluble in water (e.g., 912 g L^{-1} at 25 °C for $FeCl_3$)[76]. Upon dissolution, an acidic and stable solution forms due to the hydrolysis of Fe^{3+}/Fe^{2+} ions. The resulting acidic environment is analogous to the local pitting or crevice environment of steels. Actually, in a given pitting[77] or crevice corrosion[56] event, the local concentration of Fe^{3+}/Fe^{2+} ions can exceed 1 M due to the autocatalytic nature of the localized corrosion. A salt film is often observed on the dissolving metal surface when supersaturation is reached[78,79]. The hydrolysis of these metal cations increases the local acidity, further stabilizing these cations in a confined pit or crevice. The increase of Fe^{3+}/Fe^{2+} ion concentration is generally accompanied by the enrichment of Cl^- irons via electromigration[24]. Such a high concentration of metal cations, H^+, and Cl^- can exist locally as long as the mass transport limitation within a pit or crevice can be maintained, which might not be significantly influenced by the aeration condition of the bulk environment. The presence of iron chlorides in the solution substantially accelerated the initial glass corrosion rate by a factor of 50–70 (based on the B concentration in

solution) in the case of 0.25 M $FeCl_3$. The effect is more significant than most of the reported solid-state steel corrosion products. Additionally, all major glass components except for Si, but including U, were detectable in the leachates within three days, suggesting an acidic corrosion mechanism[74]. Indeed, the introduction of Fe cations strongly reduced the solution pH due to the hydrolysis of the Fe cations, which may partially account for the accelerated glass dissolution. However, the acceleration effect for the 0.25 M $FeCl_3$ solution was twice that of the 0.25 M HCl, so other factors should also be considered but remain unknown. Although the formation of iron-silicates has been broadly used to interpret the acceleration effect of iron on glass corrosion, the result obtained in this study does not support this mechanism, because a very low amount of iron-silicate precipitates were identified in this study. The low amount of iron-silicates detected is likely associated with the high solubility of these species in an acidic environment. The high initial dissolution rate of B—a glass alteration tracer—in 0.25 M $FeCl_3$ gradually leveled off after several months and reached a value much lower than that in DI water, while a similar trend was observed for other mobile species including Li, Na, and K. Since the leaching solution was replaced completely with an identical volume of fresh solution at given intervals, the long-term glass corrosion was not limited by the availability of Fe^{3+} and Fe^{2+} ions in this study. However, in practical scenarios, the rate of glass corrosion will depend on the amount of Fe^{3+} and Fe^{2+} ions dissolved from metallic canisters. Hence, the low long-term leaching rate of mobile species observed in this study is more likely associated with surface depletion and longer diffusion path rather than the slowing down of the net glass dissolution rate. This notion is further supported by the constantly low pH (~1) and high leaching rate of Si and Al on the order of 0.01–0.1 g m^{-2} day^{-1} (for WVDP glass in 0.25 M $FeCl_3$) throughout the one year testing period, suggesting that matrix dissolution dominated the long-term effect.

Lutze and Grambow suggested that the presence of Fe^{3+}/Fe^{2+} couple resulting from canister corrosion may also alter the redox potential of the nearfield environment[80]. As a consequence, species derived from glass corrosion, for example, TcO_4^-, could be reduced to form insoluble species. Although the hypothesized mechanism was not studied in detail by Lutze and Grambow, it is a topic of interest for glasses with redox reactive components. Indeed, De Combarieu et al. showed that Ag^+ ions, existing in a trace amount in SON68 glass, were reduced to metallic Ag in the presence of metallic Fe[26].

Glass and other metals/metal compounds

Glass corrosion can also be influenced by other materials, including but not limited to $Pb/PbO/PbO_2$, Al/Al_2O_3, Cu, Sn, and Ti. One of the earliest efforts was made by Buckwalter and Pederson, who corroded PNL 76–68 glass in containers made from Pb, Al, Cu, Ti, Sn, and Teflon in DI water at 90 °C for 28 days[81]. They found that Pb and Al substantially reduced glass corrosion, which was attributed to the considerable precipitation of Pb- and Al-rich film on glass surface. On the other hand, the effect of other materials was indistinguishable, and no precipitation was identified on the glass. The drastic difference between these materials may be associated with their different self-corrosion rates. As suggested by the authors, the corrosion of metals was only detected for Pb and Al, suggesting that the protection of glass may be at the expense of the corrosion of these metals. Interestingly, the corrosion of glass increased the concentration of soluble Pb ions by one order of magnitude, well exceeding its solubility. The authors suggested that this may be due to the complexation of Pb^{2+} cations with hydroxyl or carbonate ions. Similar inhibition effect of Pb and Al/Al_2O_3 was reported by Barkatt et al.[49], who proposed that Pb and Al/Al_2O_3 may react with silicates and form highly insoluble Pb- or Al-silicates.

Following the work by Buckwalter and Pederson[81], Kim et al. studied the influence of Pb, PbO, PbO$_2$, mixture of Fe:Pb (10:1), Cu, and Al on the corrosion of a simulated borosilicate waste glass in aerated or Ar-purged DI water[61]. The addition of Pb or PbO significantly suppressed the corrosion of glass in both aerated and Ar-purged solutions, which was attributed to the precipitation of Pb(OH)$_2$ on the glass surface. Interestingly, PbO$_2$ had a marginal effect in the aerated solution, but it clearly enhanced glass corrosion in the Ar-purged environment. Kim et al. attributed this acceleration effect to the formation of Pb-silicate precipitates, a mechanism similar to the iron-silicate precipitation. However, it is not clear why similar precipitation did not occur in the aerated condition. This interpretation is also contradictory to Barkatt et al.[49], who believed that the precipitation of Pb-silicates suppressed glass corrosion. Although it was not discussed by the authors, the distinct behavior of PbO$_2$ under different aeration conditions may be associated with its compromised stability in the reducing environment. Kim et al. also reported that a mixture of Fe and Pb at a ratio of 10:1 further reduced the corrosion rate of the glass compared to the case of pure Pb, which was attributed to the lower pH of the solution due to the presence of Fe, or the adsorption of Fe on the surface of the glass. The latter seems less likely because Fe and steel corrosion products have been known to enhance glass corrosion as mentioned above. Also, in contrast to Buckwalter and Pederson[81], Kim et al. found that Cu and Al both accelerated glass corrosion, which was ascribed to the formation of Cu- and Al-silicates, but no solid-state characterization was performed.

Apparently, there are many contradictory results within the limited literature available regarding how the materials covered in this section influence the corrosion of glass. Therefore, this is certainly another area requiring further studies.

Crystalline ceramics and metals/metal compounds

Since 1970s, crystalline ceramics have been proposed as potential waste form materials to accommodate problematic nuclear wastes that cannot be handled by glass[82,83]. Compared to the extensive works conducted on the self-corrosion of the ceramic waste forms, extremely limited studies exist with respect to the corrosion interactions between these waste forms and the metallic canister. One of the reported mechanisms among the limited studies is based on reactions between the ceramics and redox couples stemming from the corrosion of metallic canisters, such as Fe^{3+}/Fe^{2+}. This is a mechanism similar to what was hypothesized by Lutze and Grambow[80] and has been briefly reviewed in Section "Glass and aqueous Fe^{2+}/Fe^{3+} cations". For instance, Luca et al. demonstrated that the presence of aqueous Fe^{3+} enhanced the dissolution of two redox active and semiconducting ceramic waste forms (in an oxic condition), including Cs-containing hexagonal tungsten bronze and hollandite[84]. The authors suggested that the Ti^{3+} and Mo^{5+}/W^{5+} species present in the ceramics can be oxidized by aqueous Fe^{3+}, thus facilitating the structure collapse and/or ion-exchange that eventually leads to the enhanced corrosion of the ceramics. Similar redox reactions have been extensively studied between spent nuclear fuel and the corrosion products of metallic canisters in a broad range of environments[13,85–90]. Since spent fuel is not the focus of this article, these studies will not be further discussed.

Another interaction mechanism between crystalline ceramics and metals is based on the effects of metal crevice corrosion, as disclosed in recent studies by Guo et al[45,91,92]. who revealed a synergistic corrosion interaction between SS and a Cr-bearing hollandite in an oxic environment[45]. When the two materials were corroded in close proximity in Cl$^-$ bearing solutions, Cr^{3+} cations were released from both materials and the local concentration gradually built up within the confined crevice space formed by the two materials. When the Cr^{3+} concentration exceeded a specific

threshold, the self-accelerated active dissolution of SS occurred in the form of crevice corrosion, which created a highly acidified environment that rapidly corroded both the SS and hollandite substrates. In comparison, this crevice corrosion assisted attack was absent on the couple of SS and an Al-bearing hollandite, where Cr was replaced by Al. This finding suggests that the interaction depends on the hydrolysis of the released metal cations, which directly determines the aggressiveness of the crevice environment.

Ion-exchange is a dominant corrosion mechanism for various ceramic waste forms, including apatite[93], perovskite[94], and pyrochlore[95]. This process highly depends on the concentration of soluble species in the environment[96], including both cations and anions. It has been well established the local concentration of Cl$^-$ ions can be substantially increased during crevice corrosion owing to eletromigration[24]. Therefore, it is expected that the ion exchange process may be facilitated between the Cl$^-$ ions and ceramics with exchangeable anions in a crevice corrosion environment. This hypothesis was validated by Guo, Yao and their colleagues by corroding SS in close proximity to an I-bearing apatite (I-APT) in an oxic environment[91,92]. It was found that the corrosion of I-APT was enhanced by the crevice corrosion of SS, as evidenced by the increased alteration layer thickness in the crevice mouth area of the I-APT. In this specific region, I$^-$ ions originally existing in the alteration layer were clearly replaced by Cl$^-$, a process accompanied by the precipitation of nanocrystalline Cl- and I-bearing apatites. The morphology of these precipitates resembles that observed for I-APT leached in 6 M NaCl solution, validating the high concentration of Cl$^-$ present in the crevice formed by SS and I-APT. Although the corrosion of I-APT was accelerated by SS, the presence of I-APT appeared to suppress the corrosion of SS, probably by forming a protective surface film enriched in Pb and V. However, this suppression effect was self-limiting because the corrosion of I-APT was still accelerated by the crevice corrosion of SS. It should be emphasized that all studies reviewed in this section were conducted in oxic conditions and there is a lack of data for the anoxic environments. Since localized corrosion of the metallic structure is the dominant driving force for these interactions, it is expected that similar corrosion reactions might occur in an anoxic condition if localized corrosion could initiate and propagate under a given condition (irradiated conditions for example, ref. [30]). Evidently, further studies are required to better understand the interactions between metals/metal compounds and crystalline ceramic waste forms.

SUMMARY AND PERSPECTIVES

In summary, the corrosion of glass or crystalline ceramic waste forms can be influenced by close contact with a broad spectrum of materials. These interactions cause nearfield changes of the solution chemistry, which also impact the corrosion of other materials present nearby. These are complex processes governed by the structure, chemistry, formation condition, thermodynamic history, and proximity of the materials in contact, as well as the surrounding environment. Among the complicated reactions that may occur in each system, some fundamental corrosion mechanisms have been identified to be responsible for the enhanced corrosion, including but not limited to the precipitation of secondary phases, sorption of corrosion product on diverse material surfaces, acidic attack stemming from the hydrolysis of metal cations, oxidation by Fe^{3+}, and metal crevice corrosion driven attack. Generally, the corrosion of nuclear waste glass is enhanced in the presence of carbon steel, selected corrosion-resistant alloys, solid-state steel corrosion products, and aqueous Fe^{2+}/Fe^{3+} species, whereas the presence of Pb/PbO reduces glass corrosion. The effect of some other materials, such as Cu and Al, remains unclear owing to the contradictory results in the literature. Several scientific gaps have been identified in this

review and there are many open questions that need to be addressed, including (1) under which condition will the steel corrosion products have a long term accelerating effect on glass corrosion; (2) whether this long term effect will occur in the actual repository; (3) how the metallic container/overpack and the long-term corrosion products evolve during the long-lasting interactions with the backfill materials (e.g., bentonite) and the corresponding impact on the corrosion of adjacent glass or crystalline ceramic waste forms; (4) how to apply the understanding gained in short-term experiments to the geological timescale; (5) how to reliably predict and effectively control the self-accelerated corrosion interactions between dissimilar materials; (6) determination of the thermodynamic stability of the secondary phases resulting from the corrosion interactions and how it impacts the long-term durability of the waste forms and the release of radionuclides; (7) assessment of how the phenomena described above are influenced by the actual repository environment including the continuously evolving temperature and radiation field, the presence of a more complex solution chemistry, and potential microbial effects.

Another important notion is that none of the experiments carried out to date can directly simulate the actual conditions of the disposal system at any time period, because there are too many variables and processes at play. Consequently, the experiments can only focus on sub-systems and are useful for developing or improving models. It is hence crucial to systematically and quantitatively study the interactions of different materials with well-controlled or well-understood composition, structure, proximity, and thermodynamic properties in well-controlled environments, including but not limited to solution composition, temperature, pH, and radiation that bound a specific range of repository environments. Results gained through these studies can thus be fed into multiscale and multiphysics models allowing a more accurate prediction of the corrosion of the waste package. Validation of such holistic models is a key step in this respect. Although a direct validation is not feasible, partial ones can be made relying on natural or archeological analogs as well as integrated mockups or in situ experiments in underground research laboratories[97].

In addition, although the precipitation of iron-silicates has been recognized as one of the key mechanisms responsible for the enhanced glass corrosion in nearfield environments, the nature of such precipitates in a realistic environment is not yet understood and requires comprehensive characterization. The atomic- and molecular-scale understanding of the interactions between Fe^{3+}/Fe^{2+} ions and glass in aqueous environments should also be explored, which is feasible through the development of models based on density functional theory and molecular dynamics. Since the effect of Fe^{3+}/Fe^{2+} ions on glass corrosion is self-accelerated in nature due to the high tendency to hydrolyze and these cations also exist in some nuclear waste glasses (e.g., SRL and WVDP glasses) as structure components[73], it is important to investigate how these metal cations released from the glass substrate impact glass corrosion. Additionally, given the importance of localized corrosion of metallic containers, it is crucial to explore whether localized corrosion of CS or CRAs could occur in a real-world anoxic repository (e.g., in a radiation field[30]) and any subsequent influence on the alteration of glass or crystalline ceramics present nearby.

DATA AVAILABILITY

The data that support the findings of this study are available from the corresponding author upon request.

REFERENCES

1. Ojovan, M. I., Lee, W. E. & Kalmykov, S. N. *An Introduction to Nuclear Waste Immobilisation*. 326 (Elsevier, OxFord, 2019).
2. Gin, S. et al. An international initiative on long-term behavior of high-level nuclear waste glass. *Mater. Today* **16**, 243–248 (2013).
3. Kaspar, T. C. et al. Physical and optical properties of the International Simple Glass. *NPJ Mater. Degrad.* **3**, 15 (2019).
4. Pettit, N. Defense High Level Waste Disposal Container System Description Document. No. MOL. 20010927.0068 (Yucca Mountain Project, Las Vegas, Nevada (US), 2001).
5. Bridges, T., Lengyel, A., Morton, D. & Pincock, D. Standardized DOE Spent Nuclear Fuel Canister and Transportation System for Shipment to the National Repository. INEEL/CON-00-01229, *Idaho National Engineering and Environmental Laboratory* (2001).
6. Shideler, G., Reference Design Description for a Geologic Repository, Rev. 03, ICN 02. MOL–20010206-0156 (Yucca Mountain Project, 2001).
7. Gordon, G. F. N. Speller award lecture: corrosion considerations related to permanent disposal of high-level radioactive waste. *Corrosion* **58**, 811–825 (2002).
8. Dunn, D., Cragnolino, G. & Sridhar, N. An electrochemical approach to predicting long-term localized corrosion of corrosion-resistant high-level waste container materials. *Corrosion* **56**, 90–104 (2000).
9. Long, J. C. & Ewing, R. C. Yucca Mountain: Earth-science issues at a geologic repository for high-level nuclear waste. *Annu. Rev. Earth Planet Sci.* **32**, 363–401 (2004).
10. Bates, J., Bradley, J., Teetsov, A., Bradley, C. & Ten Brink, M. B. Colloid formation during waste form reaction: implications for nuclear waste disposal. *Science* **256**, 649–651 (1992).
11. Grambow, B. Geological disposal of radioactive waste in clay. *Elements* **12**, 239–245 (2016).
12. Crusset, D. et al. Corrosion of carbon steel components in the French high-level waste programme: evolution of disposal concept and selection of materials. *Corros. Eng. Sci. Technol.* **52**, 17–24 (2017).
13. Duro, L., El Aamrani, S., Rovira, M., de Pablo, J. & Bruno, J. Study of the interaction between U (VI) and the anoxic corrosion products of carbon steel. *Appl. Geochem.* **23**, 1094–1100 (2008).
14. Michelin, A. et al. Effect of iron metal and siderite on the durability of simulated archeological glassy material. *Corros. Sci.* **76**, 403–414 (2013).
15. National Research Council. *Disposition of high-level waste and spent nuclear fuel: The Continuing societal and technical challenges.* 50 (National Academies Press, Washington, DC, 2001).
16. Kursten, B. et al. J. Review of passive corrosion studies of carbon steel in concrete in the context of disposal of HLW and spent fuel in Belgium. *Proceedings of the ASME 2013 15th International Conference on Environmental Remediation and Radioactive Waste Management.* Brussels, Belgium, **1**, V001T002A027 (2014).
17. Lu, P., Kursten, B. & Macdonald, D. D. Deconvolution of the partial anodic and cathodic processes during the corrosion of carbon steel in concrete pore solution under simulated anoxic conditions. *Electrochim. Acta* **143**, 312–323 (2014).
18. Mallants, D., Marivoet, J. & Sillen, X. Performance assessment of the disposal of vitrified high-level waste in a clay layer. *J. Nucl. Mat.* **298**, 125–135 (2001).
19. Kovalov, D., Ghanbari, E., Mao, F., Kursten, B. & Macdonald, D. D. Investigation of artificial pit growth in carbon steel in highly alkaline solutions containing 0.5 M NaCl under oxic and anoxic conditions. *Electrochim. Acta* **320**, 134554 (2019).
20. Kursten, B. et al. Review of corrosion studies of metallic barrier in geological disposal conditions with respect to Belgian Supercontainer concept. *Corros. Eng. Sci. Technol.* **46**, 91–97 (2011).
21. Van Geet, M. & Weetjens, E. Strategic choices in the Belgian Supercontainer design and its treatment in a safety case. No. NEA-RWM-R–2012-3-REV. 109–114 (2012).
22. Payer, J. H., Carroll, S. A., Gdowski, G. E. & Rebak, R. B. A Framework for the Analysis of Localized Corrosion at the Proposed Yucca Mountain Repository. MOL.20060405.0074 (Yucca Mountain Project, Las Vegas, Nevada, 2006).
23. Frankel, G. S. Pitting corrosion of metals—a review of the critical factors. *J. Electrochem. Soc.* **145**, 2186–2198 (1998).
24. Kelly, R. G. Crevice corrosion. *Encycl. Electrochem.* **4**, 275 (2003).
25. Kursten, B. & Druyts, F. Methodology to make a robust estimation of the carbon steel overpack lifetime with respect to the Belgian Supercontainer design. *J. Nucl. Mat.* **379**, 91–96 (2008).
26. De Combarieu, G. et al. Glass–iron–clay interactions in a radioactive waste geological disposal: an integrated laboratory-scale experiment. *Appl. Geochem.* **26**, 65–79 (2011).
27. Smart, N. R. Corrosion behavior of carbon steel radioactive waste packages: a summary review of Swedish and UK research. *Corrosion* **65**, 195–212 (2009).
28. Smart, N., Blackwood, D. & Werme, L. Anaerobic corrosion of carbon steel and cast iron in artificial groundwaters: part 1—electrochemical aspects. *Corrosion* **58**, 547–559 (2002).

29. Brossia, C. & Cragnolino, G. Effect of environmental variables on localized corrosion of carbon steel. *Corrosion* **56**, 505–514 (2000).

30. Guo, X. et al. Reply to: How much does corrosion of nuclear waste matrices matter. *Nat. Mater.* **19**, 962 (2020).

31. Cox, G. & Roetheli, B. Effect of oxygen concentration on corrosion rates of steel and composition of corrosion products formed in oxygenated water. *Ind. Eng. Chem. Res.* **23**, 1012–1016 (1931).

32. Nasrazadani, S. & Raman, A. Formation and transformation of magnetite (Fe_3O_4) on steel surfaces under continuous and cyclic water fog testing. *Corrosion* **49**, 294–300 (1993).

33. Saheb, M., Neff, D., Dillmann, P., Matthiesen, H. & Foy, E. Long-term corrosion behaviour of low-carbon steel in anoxic environment: characterisation of archaeological artefacts. *J. Nucl. Mat.* **379**, 118–123 (2008).

34. McVay, G. L. & Buckwalter, C. Q. Effect of iron on waste-glass leaching. *J. Am. Ceram. Soc.* **66**, 170–174 (1983).

35. Cailleteau, C. et al. Insight into silicate-glass corrosion mechanisms. *Nat. Mater.* **7**, 978–983 (2008).

36. Jollivet, P. et al. Investigation of gel porosity clogging during glass leaching. *J. Non-Cryst. Solids* **354**, 4952–4958 (2008).

37. Gin, S. et al. Origin and consequences of silicate glass passivation by surface layers. *Nat. Commun.* **6**, 1–8 (2015).

38. Gin, S. et al. Dynamics of self-reorganization explains passivation of silicate glasses. *Nat. Commun.* **9**, 2169 (2018).

39. Gin, S. et al. A general mechanism for gel layer formation on borosilicate glass under aqueous corrosion. *J. Phys. Chem. C.* **124**, 5132–5144 (2020).

40. Burger, E. et al. Impact of iron on nuclear glass alteration in geological repository conditions: a multiscale approach. *Appl. Geochem.* **31**, 159–170 (2013).

41. Michelin, A. et al. Silicate glass alteration enhanced by iron: origin and long-term implications. *Environ. Sci. Technol.* **47**, 750–756 (2013).

42. Collin, M., Fournier, M., Charpentier, T., Moskura, M. & Gin, S. Impact of alkali on the passivation of silicate glass. *NPJ Mater. Degrad.* **2**, 16 (2018).

43. Dillmann, P., Gin, S., Neff, D., Gentaz, L. & Rebiscoul, D. Effect of natural and synthetic iron corrosion products on silicate glass alteration processes. *Geochim. Cosmochim. Acta* **172**, 287–305 (2016).

44. Reiser, J. et al. Glass corrosion in the presence of iron-bearing materials and potential corrosion suppressors. *MRS Online Proc. Libr* **1744**, 1–6 (2015).

45. Guo, X. et al. Self-accelerated corrosion of nuclear waste forms at material interfaces. *Nat. Mater.* **19**, 310–316 (2020).

46. Frankel, G. & Sridhar, N. Understanding localized corrosion. *Mater. Today* **11**, 38–44 (2008).

47. Burns, W., Upton, B. & Wicks, G. G. Interactions of SRP waste glass with potential canister and overpack metals. *J. Non-Cryst. Solids* **84**, 258–267 (1986).

48. Kovach, C. W. & Paulus-Kinsman, N. Materials Workshop for Nuclear Power Plants Stainless Steel and Nickel-Based Alloys, Nickel Development Institute (U.S. Nuclear Regulatory Commission, Rockville, Maryland, Sep. 9, 1999).

49. Barkatt, A., Sousanpour, W., Barkatt, A. & Boroomand, M. A. Effects of metals and metal oxides on the leaching of nuclear waste glasses. *MRS Online Proc. Libr.* **26**, 689 (1983).

50. Bates, J. K., Gerding, T. J. & Woodland, A. B. Parametric effects of glass reaction under unsaturated conditions. *MRS Online Proc. Libr.* **176**, 347 (1989).

51. Woodland, A. B., Bates, J. K. & Gerding, T. J. Parametric effects on glass reaction in the unsaturated test method. ANL-91/36 (Argonne National Lab., 1991).

52. Bates, J. K. et al. ANL Technical Support Program for DOE Environmental Restoration and Waste Management. No. ANL-95/20 (Argonne National Lab., 1995).

53. Padovani, C., Albores-Silva, O. & Charles, E. Corrosion control of stainless steels in indoor atmospheres—laboratory measurements under $MgCl_2$ deposits at constant relative humidity (Part 1). *Corrosion* **71**, 292–304 (2015).

54. Street, S. R. et al. Atmospheric pitting corrosion of 304L stainless steel: the role of highly concentrated chloride solutions. *Faraday Discuss.* **180**, 251–265 (2015).

55. Yeh, C.-P., Tsai, K.-C. & Huang, J.-Y. Effects of relative humidity on crevice corrosion behavior of 304L stainless-steel nuclear material in a chloride environment. *Metals* **9**, 1185 (2019).

56. Oldfield, J. & Sutton, W. Crevice corrosion of stainless steels: i. a mathematical model. *Brit. Corros. J.* **13**, 13–22 (1978).

57. Guo, X. et al. Near-field corrosion interactions between glass and corrosion resistant alloys. *NPJ Mater. Degrad.* **4**, 10 (2020).

58. Fournier, M., Frugier, P. & Gin, S. Effect of zeolite formation on borosilicate glass dissolution kinetics. *Procedia Earth Planet. Sci.* **7**, 264–267 (2013).

59. Inagaki, Y. et al. Effects of redox condition on waste glass corrosion in the presence of magnetite. *MRS Online Proc. Libr.* **412**, 257 (1996).

60. Jordan, N., Marmier, N., Lomenech, C., Giffaut, E. & Ehrhardt, J.-J. Sorption of silicates on goethite, hematite, and magnetite: experiments and modelling. *J. Colloid Interface Sci.* **312**, 224–229 (2007).

61. Kim, S., Lee, J.-G., Choi, J., Lee, G. & Chun, K. Effects of metals, metal oxides and metal hydroxide on the leaching of simulated nuclear waste glass. *Radiochim. Acta* **79**, 199–206 (1997).

62. Neill, L. et al. Various effects of magnetite on international simple glass (ISG) dissolution: implications for the long-term durability of nuclear glasses. *NPJ Mater. Degrad.* **1**, 1 (2017).

63. Bart, G. et al. Borosilicate glass corrosion in the presence of steel corrosion products. *MRS Online Proc. Libr.* **84**, 459 (1986).

64. Werme, L. et al. Chemical corrosion of highly radioactive borosilicate nuclear waste glass under simulated repository conditions. *J. Mater. Res.* **5**, 1130–1146 (1990).

65. Philippini, V., Naveau, A., Catalette, H. & Leclercq, S. Sorption of silicon on magnetite and other corrosion products of iron. *J. Nucl. Mat.* **348**, 60–69 (2006).

66. Schlegel, M. L. et al. Alteration of nuclear glass in contact with iron and claystone at 90 °C under anoxic conditions: characterization of the alteration products after two years of interaction. *Appl. Geochem.* **70**, 27–42 (2016).

67. Rebiscoul, D. et al. Reactive transport processes occurring during nuclear glass alteration in presence of magnetite. *Appl. Geochem.* **58**, 26–37 (2015).

68. Godon, N., Gin, S., Rebiscoul, D. & Frugier, P. SON68 glass alteration enhanced by magnetite. *Procedia Earth Planet. Sci.* **7**, 300–303 (2013).

69. Grambow, B., Zwicky, H., Bart, G., Bjorner, I. & Werme, L. Modeling of the effect of iron corrosion products on nuclear waste glass performance. *MRS Online Proc. Libr.* **84**, 471 (1986).

70. Jollivet, P., Minet, Y., Nicolas, M. & Vernaz, É. Simulated alteration tests on non-radioactive SON 68 nuclear glass in the presence of corrosion products and environmental materials. *J. Nucl. Mat.* **281**, 231–243 (2000).

71. Frugier, P., Chave, T., Gin, S. & Lartigue, J.-E. Application of the GRAAL model to leaching experiments with SON68 nuclear glass in initially pure water. *J. Nucl. Mat.* **392**, 552–567 (2009).

72. Fournier, M., Frugier, P. & Gin, S. Application of GRAAL model to the resumption of International Simple Glass alteration. *NPJ Mater. Degrad.* **2**, 21 (2018).

73. Pan, Y.-M., Jain, V. & Pensado, O. Degradation of high-level waste glass under simulated repository conditions. *J. Non-Cryst. Solids* **319**, 74–88 (2003).

74. Jain, V. & Pan, Y. Performance of surrogate high-level waste glass in the presence of iron corrosion products. No. INIS-FR—2903 (Center for Nuclear Waste Regulatory Analyses, 2004).

75. Baes, C. F. Jr. & Mesmer, R. Thermodynamics of cation hydrolysis. *Am. J. Sci.* **281**, 935–962 (1981).

76. Haynes, W. M. *CRC handbook of chemistry and physics*. 92nd edn, 4.69 (CRC press, Boca Raton, 2011).

77. Mankowski, J. & Szklarska-Smialowska, Z. Studies on accumulation of chloride ions in pits growing during anodic polarization. *Corros. Sci.* **15**, 493–501 (1975).

78. Rayment, T. et al. Characterisation of salt films on dissolving metal surfaces in artificial corrosion pits via in situ synchrotron X-ray diffraction. *Electrochem. Commun.* **10**, 855–858 (2008).

79. Li, T. et al. Cryo-based structural characterization and growth model of salt film on metal. *Corros. Sci.* **174**, 108812 (2020).

80. Lutze, W. & Grambow, B. The effect of glass corrosion on near field chemistry. *Radiochim. Acta* **58**, 3–8 (1992).

81. Buckwalter, C. & Pederson, L. Inhibition of nuclear waste glass leaching by chemisorption. *J. Am. Ceram. Soc.* **65**, 431–436 (1982).

82. McCarthy, G. J. High-level waste ceramics: materials considerations, process simulation, and product characterization. *Nucl. Technol.* **32**, 92–105 (1977).

83. Ringwood, A., Kesson, S., Ware, N., Hibberson, W. & Major, A. Immobilisation of high level nuclear reactor wastes in SYNROC. *Nature* **278**, 219–223 (1979).

84. Luca, V., Zhang, Y., Drabarek, E. & Chronis, H. Cesium release from tungstate and titanate waste form materials in simulated canister corrosion product-containing solutions. *J. Am. Ceram. Soc.* **90**, 2510–2516 (2007).

85. Liger, E., Charlet, L. & Van Cappellen, P. Surface catalysis of uranium (VI) reduction by iron (II). *Geochim. Cosmochim. Acta* **63**, 2939–2955 (1999).

86. Johnson, L. & Smith, P. The interaction of radiolysis products and canister corrosion products and the implications for spent fuel dissolution and radionuclide transport in a repository for spent fuel. No. NEA-RWM-R–2012-3-REV (National Cooperative for the Disposal of Radioactive Waste (NAGRA), 2000).

87. O'Loughlin, E. J., Kelly, S. D., Cook, R. E., Csencsits, R. & Kemner, K. M. Reduction of uranium (VI) by mixed iron (II)/iron (III) hydroxide (green rust): formation of UO_2 nanoparticles. *Environ. Sci. Technol.* **37**, 721–727 (2003).

88. Behrends, T. & Van Cappellen, P. Competition between enzymatic and abiotic reduction of uranium (VI) under iron reducing conditions. *Chem. Geol.* **220**, 315–327 (2005).

89. Jeon, B.-H., Dempsey, B. A., Burgos, W. D., Barnett, M. O. & Roden, E. E. Chemical reduction of U (VI) by Fe (II) at the solid− water interface using natural and synthetic Fe (III) oxides. *Environ. Sci. Technol.* **39**, 5642–5649 (2005).

90. Ewing, R. C. Long-term storage of spent nuclear fuel. *Nat. Mater.* **14**, 252–257 (2015).

91. Guo, X. et al. Corrosion interactions between stainless steel and lead vanado-iodoapatite nuclear waste form part I. *NPJ Mater. Degrad.* **4**, 13 (2020).

92. Yao, T. et al. Corrosion Interactions between Stainless Steel and Lead Vanado-Iodoapatite Nuclear Waste Form Part II. *NPJ Mater. Degrad.* **4**, 15 (2020).

93. Zhang, Z. et al. Mechanism of iodine release from iodoapatite in aqueous solution. *RSC Adv.* **8**, 3951–3957 (2018).

94. Nedelcu, G. et al. Fast anion-exchange in highly luminescent nanocrystals of cesium lead halide perovskites (CsPbX$_3$, X= Cl, Br, I). *Nano Lett.* **15**, 5635–5640 (2015).

95. Ewing, R. C., Weber, W. J. & Lian, J. Nuclear waste disposal—pyrochlore (A$_2$B$_2$O$_7$): Nuclear waste form for the immobilization of plutonium and "minor" actinides. *J. Appl. Phys.* **95**, 5949–5971 (2004).

96. Zhang, Z. et al. Effect of solution chemistry on the iodine release from iodoapatite in aqueous environments. *J. Nucl. Mat.* **525**, 161–170 (2019).

97. Poinssot, C. & Gin, S. Long-term behavior science: the cornerstone approach for reliably assessing the long-term performance of nuclear waste. *J. Nucl. Mat.* **420**, 182–192 (2012).

AUTHOR CONTRIBUTIONS

X.G. conducted literature survey and wrote the paper with help editing from S.G. and G.S.F. All authors approved the content in its current form.

COMPETING INTERESTS

The authors declare no competing interests.

ADDITIONAL INFORMATION

Correspondence and requests for materials should be addressed to X.G.

Reprints and permission information is available at http://www.nature.com/reprints

Publisher's note Springer Nature remains neutral with regard to jurisdictional claims in published maps and institutional affiliations.